


Oocyte-specific EXOC5 expression is required for mouse oogenesis and folliculogenesis

Hongwen Wu^{1,2}, Hieu Nguyen^{1,2}, Prianka H. Hashim³, Ben Fogelgren^{1,2}, Francesca E. Duncan ³, and W. Steven Ward ^{1,2,*}

¹Department of Anatomy, Biochemistry & Physiology, Institute for Biogenesis Research, John A. Burns School of Medicine, University of Hawaii at Manoa, Honolulu, HI, USA

²Department of Obstetrics, Gynecology & Women's Health, John A. Burns School of Medicine, University of Hawaii at Manoa, Honolulu, HI, USA

³Department of Obstetrics and Gynecology, Feinberg School of Medicine, Northwestern University, Chicago, IL, USA

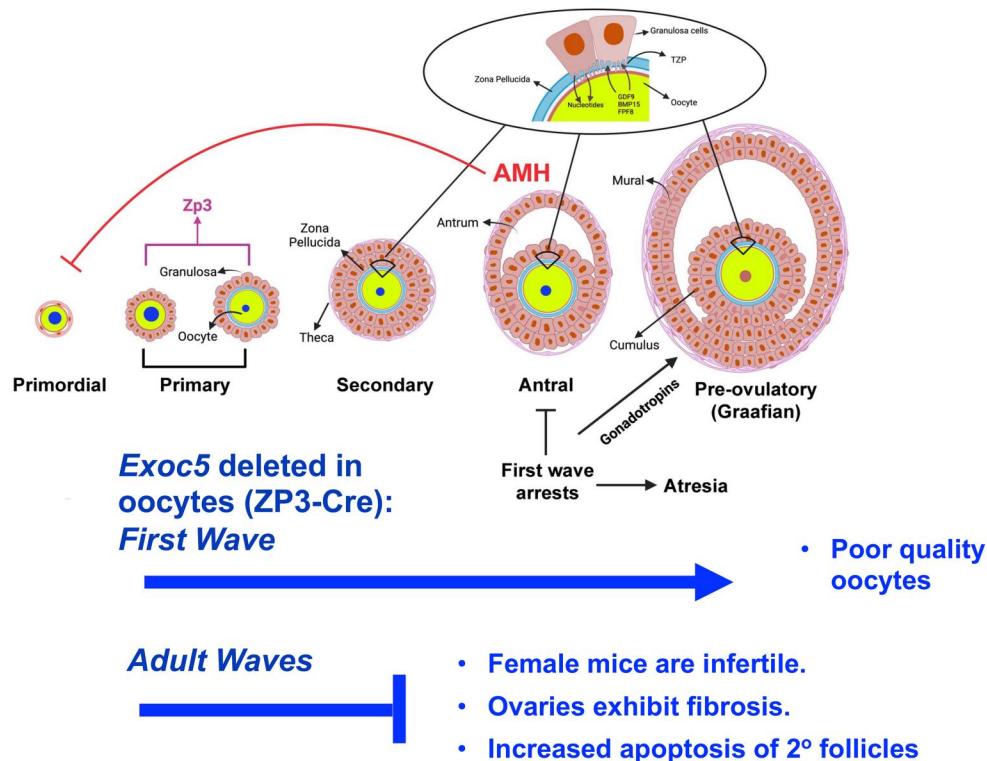
*Correspondence address. Department of Anatomy, Biochemistry & Physiology, Institute for Biogenesis Research, John A. Burns School of Medicine, University of Hawaii at Manoa, 1960 East-West Road, Honolulu, HI 96822, USA. E-mail: wward@hawaii.edu  <https://orcid.org/0000-0002-5025-192X>

ABSTRACT

EXOC5 is a crucial component of a large multi-subunit tethering complex, the exocyst complex, that is required for fusion of secretory vesicles with the plasma membrane. *Exoc5* deleted mice die as early embryos. Therefore, to determine the role of EXOC5 in follicular and oocyte development, it was necessary to produce a conditional knockout (cKO), *Zp3-Exoc5-cKO*, in which *Exoc5* was deleted only in oocytes. The first wave of folliculogenesis appeared histologically normal and progressed to the antral stage. However, after IVF with normal sperm, oocytes collected from the first wave (superovulated 21-day-old cKO mice) were shown to be developmentally incompetent. Adult follicular waves did not progress beyond the secondary follicle stage where they underwent apoptosis. Female cKO mice were infertile. Overall, these data suggest that the first wave of folliculogenesis is less sensitive to oocyte-specific loss of *Exoc5*, but the resulting gametes have reduced developmental competence. In contrast, subsequent waves of folliculogenesis require oocyte-specific *Exoc5* for development past the preantral follicle stage. The *Zp3-Exoc5-cKO* mouse provides a model for disrupting folliculogenesis that also enables the separation between the first and subsequent waves of folliculogenesis.

Keywords: folliculogenesis / EXOC5 / ovarian development / follicular apoptosis / ovarian fibrosis / female infertility

GRAPHICAL ABSTRACT



Oocyte-specific deletion of *Exoc5* results in poor-quality oocytes in the first wave of folliculogenesis and complete inhibition of folliculogenesis in all subsequent waves; the ovaries exhibit early fibrosis and the females are infertile.

Received: May 10, 2024. Revised: July 11, 2024. Editorial decision: July 17, 2024.

© The Author(s) 2024. Published by Oxford University Press on behalf of European Society of Human Reproduction and Embryology.

This is an Open Access article distributed under the terms of the Creative Commons Attribution-NonCommercial License (<https://creativecommons.org/licenses/by-nc/4.0/>), which permits non-commercial re-use, distribution, and reproduction in any medium, provided the original work is properly cited. For commercial re-use, please contact journals.permissions@oup.com

Introduction

Folliculogenesis is the process by which follicles (the functional unit of the ovary composed of oocytes surrounded by companion granulosa cells) develop to produce fertilization-competent eggs (Peters, 1969; Peters et al., 1975). Mouse females are born with a finite and nonreplenishable number of primordial follicles which make up the follicular reserve (Kerr et al., 2006). The number of primordial follicles determines the reproductive lifespan of an individual. Primordial follicles contain nongrowing primordial oocytes surrounded by a layer of flattened pregranulosa somatic cells. They constitute a postnatal pool of nongrowing follicles from which cohorts are continually recruited to undergo dramatic growth and development until the supply is exhausted. When recruited for further development, the oocytes within the developing follicles grow to more than 100-fold in size and are highly active both transcriptionally and translationally (Lewandoski et al., 1997; de Vries et al., 2000; Ploutarchou et al., 2015). During follicular development, somatic cells that surround the growing oocyte proliferate and differentiate into two types of granulosa cells: mural granulosa cells associated with a basal lamina forming the follicular wall, and cumulus cells that communicate with the central oocyte. A fluid-filled area between mural and cumulus cells is referred to as the antrum. In sexually mature females, luteinizing hormone (LH) stimulates meiotic maturation of the fully grown oocytes surrounded by cumulus cells in preovulatory (Graafian) follicles, leaving the mural granulosa cells to form the progesterone-producing corpus luteum (Channing et al., 1980; McGee and Hsueh, 2000).

In mice, the first wave of follicular activation and growth begins during the first postnatal week, but additional cohorts undergo activation continually thereafter throughout reproductive life. The pool of primordial follicles becomes gradually depleted, and few remain in the ovaries of aged females. Most of the antral follicles from the first wave undergo degeneration by 4–5 weeks of age in mice. These are gradually replaced by ongoing folliculogenesis, and ovulatory cycles begin in mice by approximately 6 weeks of age, the age of reproductive hormone-dependent cyclicity. Although they have different fates, ovulation or not, little is known about the functional differences between the first and subsequent waves of developing follicles.

Follicular development requires highly coordinated growth of the oocyte and granulosa cells with a complex metabolic cooperativity directed through bidirectional communication. The oocyte secretes paracrine factors, including GDF-9, FGF8, and BMP-15, which signal to the granulosa cells (Matzuk et al., 2002; Su et al., 2004). In turn, the oocyte's companion granulosa cells provide the oocyte with nutrients (Sugiura and Eppig, 2005; Sugiura et al., 2005; Su et al., 2008) and signals, such as cGMP which maintains meiotic arrest (Norris et al., 2009). One mechanism by which granulosa cells mediate this communication with the oocyte is through filopodia-like structures termed transzonal projections (TZPs) that extend from the cumulus cells through the zona pellucida to form physical connections with the oocyte (Clarke, 2018a,b). TZPs terminate at the oocyte via gap junctions and cadherin-mediated attachments at the sites of integration with the oocyte. The role of the exocyst complex in membrane trafficking, cell signaling, and cadherin deposition (required for gap junction formation) (Yeaman et al., 2004; Polgar and Fogelgren, 2018) suggests that it might play a role in interactions between the granulosa cells and the oocyte during folliculogenesis. Therefore, the goal of this study was to test the hypothesis that the oocyte-derived exocyst complex is required for folliculogenesis.

Originally discovered in yeast and highly conserved in mammals, the exocyst complex comprises eight proteins (EXOC1–8) and regulates the polarized exocytosis of secretory vesicles via the plasma membrane (Novick and Schekman, 1979; Novick et al., 1980). The contents of the exocyst-regulated vesicles, such as transmembrane or secreted proteins, can vary widely depending on the cell type and are often required for proper cell differentiation, physiology, or communication. Exocyst activity is largely regulated through control of the holocomplex assembly and subcellular localization by a network of small GTPases and kinases. Vesicle specificity arises from the direct binding of the EXOC6 subunit only to certain activated Rab GTPases on transport vesicles (Lepore et al., 2018; Polgar and Fogelgren, 2018). The EXOC5 subunit connects EXOC6 with the other exocyst subunits, making EXOC5 an excellent target for studies of loss-of-function of the entire exocyst complex.

Both genetic knockout and RNA-based knockdown of EXOC5 have resulted in functional disruption of exocyst activity and protein degradation of other subunits (Zuo et al., 2009; Fogelgren et al., 2011; Lee et al., 2016). Global knockout of exocyst genes in mice results in early embryonic lethality (Friedrich et al., 1997), so conditional *Exoc5* knockout strain using Cre-lox technology has been necessary to successfully inactivate exocyst trafficking in specific tissues, including the kidney (Fogelgren et al., 2015; Polgar et al., 2015; Nihalani et al., 2019), skeletal muscle (Fujimoto et al., 2019, 2021), eye (Lobo et al., 2017; Rohrer et al., 2021), inner ear (Lee et al., 2018), and heart (Fulmer et al., 2019). To study the role of the exocyst complex specifically during mammalian ovarian follicle development, an oocyte-specific conditional knockout (cKO) was produced using a Cre driven by the oocyte-specific *Zp3* promoter. This construct eliminates expression in oocytes during the earliest stages of growth beyond the primordial oocyte stage (Fogelgren et al., 2015). This loss-of-function model resulted in female infertility. Folliculogenesis was completely blocked past the preantral follicle stage between 40- and 60-day postpartum (dpp), and the ovaries exhibited accelerated aged ovarian phenotypic characteristics. Before this, the first wave of folliculogenesis appeared morphologically normal, but the resulting oocytes exhibited impaired embryonic developmental competence. These results demonstrate that oocyte-derived EXOC5 is required for fertility due to an essential role in folliculogenesis and oogenesis. Considering the known exocytic functions of EXOC5, we propose a role for oocyte-derived exosomes in folliculogenesis. Known bidirectional communication between oocytes and companion granulosa cells implicates negative effects of oocyte-derived exosomes on granulosa cell function and suggests that this, in turn, adversely affects the developmental competence of the oocyte itself.

Materials and methods

Animal care

All animal care and experimental protocols for handling and the treatment procedures reported here were reviewed and approved by the Institutional Animal Care and Use Committee at the University of Hawaii.

Breeding scheme to obtain *Zp3-Exoc5-cKO* mice

We previously generated *Exoc5^{Flox/Flox}* mice (Fogelgren et al., 2015) which were used for this study. This mouse has loxP sites flanking exons 7–10, and removal of these exons results in a frameshift with a premature stop codon. To create the cKO in which *Exoc5* was inactivated only in oocytes, we crossed *Exoc5^{Flox/Flox}* females with *Zp3-Cre^{+/+}* mice obtained from The Jackson

Laboratory (strain C57BL/6-Tg(Zp3-cre)93Kw/J) using a well-established protocol (de Vries et al., 2000; Sun et al., 2008). The final mice used in this study had the genotype *Exoc5*^{-/-}; *Zp3-Cre*^{+/-}, hereafter designated as cKO mice. Females of this genotype have no active *Exoc5* genes in the oocytes.

In situ hybridization (RNAScope) and quantification

Exoc5 mRNA transcripts were identified in ovaries from 28 to 42 dpp B6 and cKO mice using RNAScope (Advanced Cell Diagnostics, Hayward, CA, USA), an in situ mRNA hybridization technique (Wang et al., 2012). For each group, 10 ovaries from 5 individual knockout mice and 8 ovaries from 4 distinct B6 mice (with 2 ovaries per mouse and 4 sections per mouse) underwent separate hybridizations with both long and short probes. Peptidylprolyl isomerase (PIIB) (Advanced Cell Diagnostics) served as the positive control according to the manufacturer's recommendation. All probes were sourced from the same manufacturer, with the RNAScope 2.5 HD Red assay kit employed for signal amplification and detection. The experimental procedure involved de-paraffinization of ovarian sections, followed by probe hybridization, target retrieval, signal amplification, and signal detection. High-quality images were captured using an EVOS FL Auto Imaging System (Thermo Fisher Scientific, Waltham, MA, USA) equipped with 20× and 40× objectives. Signal quantification was conducted using Fiji ImageJ software (National Institutes of Health, Bethesda, MD, USA), wherein color deconvolution was performed based on the signal from the positive PIIB control image, serving as the standard reference. The positive signal of each follicle was then accentuated using threshold adjustment tools, with the percentage of positive signal recorded for each oocyte and surrounding granulosa cells individually.

Single oocyte PCR

A single cKO GV oocyte or an *Exoc5*^{Flox/Flox} control oocyte was added to a PCR tube (Thermo Fisher Scientific) containing 4 μl of GNTK buffer (50 mM KCl, 1.5 mM MgCl₂, 10 mM Tris, pH 8.5, 0.45% Triton X-100, 0.45% Tween 20) supplemented with 100 μg/ml proteinase K. These tubes were incubated at 55 °C for 2.5 h with a BioRAD C100 Touch thermocycler (BioRAD Laboratories, Inc, Hercules, CA, USA) to extract total DNA. These DNA tubes were directly used to perform PCR by using a KOD hot Start DNA Polymerase kit (Millipore/Sigma, Burlington, MA, USA). The primers used were CKO-F and CKO-R (Supplementary Table S1). The PCR amplification reactions were performed using a BioRAD C1000 Touch thermocycler. The PCR cycle protocol consisted of 2 min hold at 95 °C, followed by 35 cycles of 10 s at 98 °C, 30 s at 60 °C, and 2 min at 72 °C, and then following cycling with a final step for 5 min at 72 °C. The PCR products were then run on 1% agarose gels supplemented with ethyl bromide. Gels were imaged using the Fujifilm LAS-3000 imager (Fujifilm Corporation, Tokyo, Japan). Primers are shown in Supplementary Table S1.

Quantitative RT-PCR

Total RNA from 100 cKO metaphase II (MII) oocytes was extracted and purified by using TRizol & Trace kit (Thermo Fisher Scientific). cDNA was then synthesized from this total RNA by reverse transcription of polyadenylated RNA using Superscript Reverse Transcriptase IV following manufacturer's protocols (Thermo Fisher Scientific). Then, RT-PCR was performed using SYBR Green PCR Master Mix on an ABI Step-OnePlus machine (Applied Biosystems, Carlsbad, CA, USA). RT-PCR reactions were performed at 95 °C for 10 min followed by 35 PCR cycles (10 s at 95 °C and 60 s

at 60 °C) (Supplementary Table S2). All reactions were performed in triplicate per assay, and *β-actin* was included in every PCR reaction as a loading control. The different values in PCR cycles regarding *β-actin* for a given experimental sample were subtracted from the mean Δ Ct of the reference samples (*Exoc5*^{Flox/Flox}) ($\Delta\Delta$ Ct) (Livak and Schmittgen, 2001; Schmittgen and Livak, 2008). The quantification of *Exoc5* knockdown values was further normalized to $\Delta\Delta$ Ct values of the *β-actin*.

Fertility assessment of female mice

Fertility assessments were conducted by pairing three sets of *Exoc5*^{Flox/Flox} *ZP3-Cre*^{+/-} females with C57BL/6 (B6) males. As a control, three pairs of males with the identical genotype profiles (*Exoc5*^{Flox/Flox} *ZP3-Cre*^{+/-}) were mated with B6 females. The average litter size was recorded 21-day post-mating. Following this initial assessment, the *Exoc5*^{Flox/Flox} *ZP3-Cre*^{+/-} female groups were continuously mated with B6 males for an extended period of three additional months to further test their fertility.

Ovarian histology and follicle classification and counting

Ovaries were collected and fixed in Modified Davidson's fixative for 3 h at room temperature and then transferred to 4 °C overnight with gentle agitation. Tissues were then washed in 70% EtOH three times for 10 min. The ovaries were then embedded in paraffin and serial sectioned at 5 μm thickness. The first section that had tissue and every subsequent fifth section were placed on slides designated for follicle counting. All the follicle-counting slides were stained with hematoxylin and eosin according to standard protocols. Healthy follicles with normal morphology were classified by developmental stage according to established morphological criteria (Duncan et al., 2017). A primordial follicle was defined as an oocyte surrounded by a single complete or incomplete layer of squamous granulosa cells. A primary follicle was defined as an oocyte surrounded by a single layer of cuboidal granulosa cells. A secondary follicle was defined as an oocyte surrounded by multiple layers of cuboidal granulosa cells. Early antral follicles were characterized by multiple layers of granulosa cells and developing fluid-filled spaces. Antral follicles were characterized by a single large continuous fluid-filled cavity, and a clear cumulus-oocyte complex that was distinct from the granulosa cell layer. Corpora lutea were identified by the presence of characteristic hypertrophied luteinized cells with a larger cytoplasmic:nuclear ratio relative to other cells in the ovary. Atretic follicles were characterized by a misshapen oocyte and/or dark, pyknotic granulosa cells. Follicles were classified and counted according to these criteria for both ovaries from three mice across genotype and age. The follicle counts were reported as the average number of follicles per section for each ovary.

TUNEL analysis

We followed the manufacturer's protocol for the DeadEnd™ Fluorometric TUNEL System (Promega, Madison, WI, USA) to detect apoptosis cells. Paraffin-embedded histology sections were deparaffinized with xylene, washed, and rehydrated in decreasing concentrations of ethanol (100%, 95%, 85%, 70%, 50%). Then slides were immersed in 0.85% NaCl for 5 min before fixing slides with 4% formaldehyde in PBS in 15 min. The slides were permeabilized with proteinase K for 8–10 min, washed in PBS for 5 min, repeated fix with 4% formaldehyde in PBS in 5 min, and washed again in PBS for 5 min. Finally, we performed TUNEL staining. We equilibrated and labeled with TdT transferase at 37 °C for 1 h in the dark. The reaction was stopped by 2x saline sodium citrate (SSC buffer). The slides were washed three times with PBS and

were counterstained with VECTASHIELD Antifade with DAPI (Vector Laboratories, Inc, Newark, CA, USA). The slides were imaged using a fluorescent Olympus DP80 microscope. Image analysis was performed by ImageJ. Quantification of positive signal was established by using the method from Keith R. Porter Imaging Facility at the University of Maryland, Baltimore County (<https://kpf.umbc.edu/image-processing-resources/imagej-fiji/termining-fluorescence-intensity-and-area/>). Briefly, the fluorescence-positive signal was identified using the Color Threshold tool in ImageJ. To establish background levels, the intensity of three distinct areas within each image that had no visible fluorescent signal were averaged. Subsequently, individual follicles were selected using the region of interest tool. The intensity of each follicle was measured, and the corrected total cell fluorescence was computed by subtracting the background intensity from the area-adjusted follicle intensity. Finally, the percentage of positive signal was calculated. Transcripts were normalized per follicle.

Collagen staining and analysis

To assess collagen I and III, we performed histological staining using Picrosirius Red (PSR) following previously published methods (Briley et al., 2016; Amargant et al., 2020). Briefly, histologic sections were deparaffinized with CitriSolv three times for 3 min each, washed, and rehydrated in decreasing concentrations of ethanol (100%, 70%, 30%, and ddH₂O) for 1 min each. The slides were immersed in PSR solution (0.1% Sirius Red F3b and 1.3% saturated aqueous solution of picric acid) for 40 min and in 0.005 N HCl in H₂O for 1.5 min. The slides were rehydrated in 100% EtOH three times for 30s and cleared with CitriSolv (Citra Solv LLC, Danbury, CT, USA) for 5 min. The slides were then mounted using Cytoseal (Citra Solv LLC), and the slides were imaged using the EVOS FL Auto cell imaging system. To measure the percentage of PSR-positive signal, we employed the threshold tool in ImageJ. This tool allowed us to quantify the area exhibiting positive PSR staining above a threshold, which was determined by reference to the staining observed in the oldest animal ovarian section. Consistency was maintained by keeping this threshold constant across all images analyzed for each specific mouse ovarian section (Briley et al., 2016).

IVF and assessment of embryo development

Spermatozoa were collected from 8- to 10-week-old B6 male mice sourced from Charles River (Wilmington, MA, USA). The caudal epididymis was dissected to release sperm into HTF medium (100 mM NaCl, 4.7 μM KCl, 200 mM MgSO₄, 400 μM KH₂PO₄, 5 nM CaCl₂, 2.77 mM glucose, 16 μM sodium lactate, 336 μM sodium pyruvate, 200 μM penicillin G, 70 μM streptomycin, 25 mM NaHCO₃, 0.01% phenol red, and 4 mg/ml BSA). The sample was then incubated at 37 °C and 5% CO₂ for 1 h in a 1.5-ml tube to allow sperm dispersion. Post-incubation, the motile sperm were prepared for IVF. For IVF, mature MII oocytes were harvested from 21 dpp superovulated females which received 5 IU each of eCG and hCG 48 h apart. The oviducts were excised 14- to 15-h post-hCG injection and maintained in light mineral oil (Irvine, Newport Beach, CA, USA). MII oocytes, encircled with cumulus cells, were retrieved, and combined with motile sperm in a prewarmed drop of HTF medium for a 6-h incubation. After fertilization, the zygotes were cultured in Global Total media (LifeGlobal, LGGT-30, Guilford, CT, USA) until they reached the blastocyst stage.

Parthenogenetic egg activation

Control MII eggs from normal B6 mice were incubated in calcium-free CZB medium supplemented with 10 mM SrCl₂ and

10 ng/ml cytochalasin B (CB) for 3 h, then the activated oocytes were transferred into Global Total media. For cKO, MII eggs underwent a similar treatment, but in CZB medium containing calcium and 10 ng/ml CB for at least 3 h. Both control and cKO-activated eggs were then cultured at 37 °C in a humidified 5% CO₂ atmosphere until they developed to the 2-cell stage.

Statistical analysis

We used GraphPad Prism version 8.3.1 (GraphPad Software, La Jolla, CA, USA) for graph plotting and statistical analysis. To assess the normal distribution of the data, we employed the Shapiro–Wilk and Kolmogorov–Smirnov tests. Analysis between groups of continuous variables was performed with Student's *t*-test or Mann–Whitney *U*-test depending on data distribution. Significant differences were indicated by a *P*-value <0.05. Variability within the experimental group is presented as the SEM.

Results

Exoc5 expression in the ovary

To determine the expression pattern of *Exoc5* in the ovary, and particularly within the ovarian follicle, we performed *in situ* hybridization for *Exoc5* mRNA. We generated a probe to evaluate *Exoc5* mRNA expression (Supplementary Fig. S1). Mouse *Exoc5* has 18 exons. Our probe covered exons 4–12 (1026 bp) and included 5 exons that are not deleted. *Exoc5* was expressed in both the oocytes and surrounding granulosa cells at all follicle stages, including primordial, primary, secondary, and antral follicles (Fig. 1A). The level of *Exoc5* expression was the same in primary, secondary, and antral follicles in control ovaries with no statistical differences noted (Fig. 1C, Supplementary Fig. S2A). We did not quantify the levels of *Exoc5* expression in primordial follicles, but Fig. 1Aa demonstrates that expression was observed. The expression of *Exoc5* in both oocytes and granulosa cells in all stages of follicle development suggests that EXOC5 functions throughout folliculogenesis.

Verification of *Exoc5* deletion in cKO oocytes

To investigate the function of *Exoc5* in the ovary, we generated a cKO model in which *Exoc5* was specifically removed from oocytes. We have previously used the *Zp3-Cre* system and demonstrated by single oocyte PCR that it deletes the floxed gene of interest in oocytes beginning at the primary follicle stage (Nguyen et al., 2022). We created *Zp3-Exoc5*-cKO mice using this system and verified by single oocyte PCR that exons 7–10 of the *Exoc5* gene were deleted in *Zp3-Exoc5*-cKO oocytes isolated from antral follicles of 28 dpp mice (Supplementary Fig. S3). The deletion of these exons creates a gene that prematurely terminates transcription with a frameshift mutation, inactivating *Exoc5* (Fogelgren et al., 2015). Only cKO oocytes had *Exoc5* deletions, whereas neither *Exoc5*^{Flox/Flox} or control (B6 wild type) oocytes had deletions. We also verified by RT-PCR that no intact *Exoc5* mRNA survived to the antral follicle stage in cKO oocytes (Supplementary Fig. S4). We also confirmed the cKO in histological sections using RNA *in situ* hybridization (Fig. 1B–D). In cKO ovaries, there were minimal transcripts in the oocytes relative to controls, but there were still transcripts present in the surrounding granulosa cells as expected for an oocyte-specific KO (Fig. 1B and D, Supplementary Fig. S2). We further verified this by creating a second, shorter ISH probe that only contained the four exons that were excised. This signal was much lower, but also demonstrated that *Exoc5* was not expressed in oocytes of cKO mice (Supplementary Fig. S2A). Of note, although *Exoc5* was still

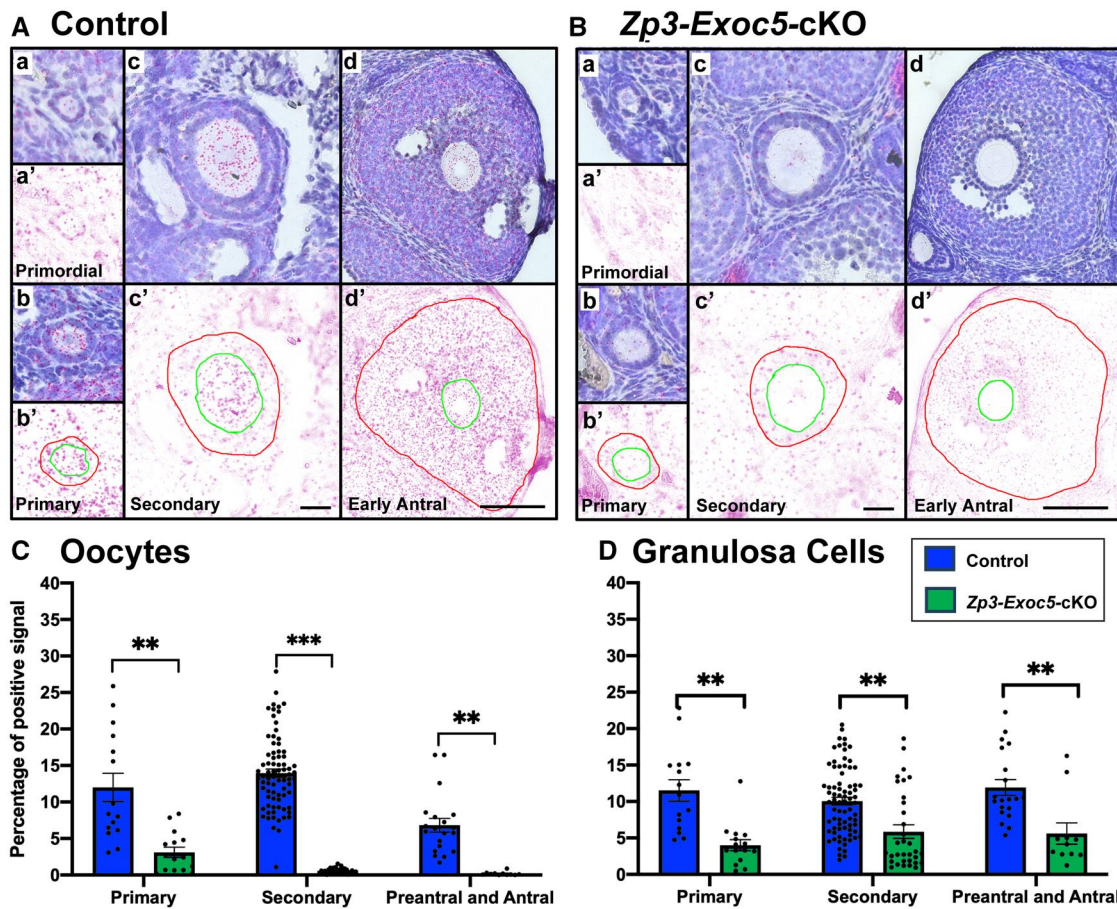


Figure 1. Expression of *Exoc5* in control and knockout (cKO) ovaries. (A) Histological sections of control of 30 days postpartum (dpp) ovaries stained for *Exoc5* mRNA expression with *in situ* hybridization. One example, each, of a primordial (a), primary (b), secondary (c), and early antral follicle (d) are shown. *Exoc5* RNA signals are red dots. Each image was deconvoluted to emphasize the RNA signals with a green circle marking the ovary and a red circle marking the outer rim of the granulosa cells (a' through d'). (B) Exactly as in (A), except the ovaries were obtained from cKO (*Zp3-Exoc5-cKO*) mice. All images in (A) and (B), a through c' are shown at the same magnification (bar = 25 μ m) and in (A) and (B), d and d' (bar = 100 μ m). (C and D) Quantification of the RNAScope signals in oocytes is shown for (C) oocytes and (D) granulosa cells. Each dot represents one oocyte in the follicles of the type indicated. All ages of mice were combined in this graph.

expressed in the granulosa cells within follicles from cKO mice, the transcript numbers were reduced compared to WT controls (Fig. 1D, Supplementary Fig. S2B). Because the *Zp3* promoter is not active in granulosa cells, the *Exoc5* gene is not expected to be deleted in these cells. Thus, the observed reduction may be due to loss of EXOC5 in the oocytes resulting in impaired cell-cell communication.

cKO females are infertile

To determine whether oocyte-specific deletion of *Exoc5* impacts reproductive function, we compared the fertility of adult (42 dpp) cKO females mated with normal, B6 males with that of three pairs of *Exoc5^{Flox/Flox}; Zp3-Cre^{+/-}* males mated with normal B6 females (N = 3 breeding pairs/genotype). *Exoc5^{Flox/Flox}; Zp3-Cre^{+/-}* males were produced in the same litters as the cKO females but have normal reproductive function, since *Zp3-Cre* is not activated in male mice. *Exoc5^{Flox/Flox}; Zp3-Cre^{+/-}* males mated with control females produced a total of 24 pups (average of 8 pups/ breeding pair), whereas only one pup, which died 24 h after birth, was born from all breeding pairs of cKO females and normal B6 males (Table 1). Thus, cKO females were infertile, whereas males of the same genotype were fertile.

Table 1. Female *Zp3-Exoc5-cKO* are infertile.^a

Mouse genotypes	Exp. No.	No. pups
Female <i>Zp3-Exoc5-cKO</i>	1	0
×	2	1 (died dpp 1)
Male B6	3	0
Female B6	1	9
×	2	7
Male <i>Exoc5^{Flox/Flox}; Zp3-Cre^{+/-}</i>	3	8

^a For mating experiments, 6-week-old mice were housed together for 12 weeks and the females were checked weekly for pregnancies. For female cKO fertility, a male control (B6) was housed with a female *Zp3-Exoc5-cKO* mouse for 12 weeks (three matings were performed). Males with the same genotype as *Zp3-Exoc5-cKO* females were *Exoc5^{Flox/Flox}; Zp3-Cre^{+/-}* but were not conditional knock-outs because *Zp3-Cre* is not activated in males. These males were mated with control (B6) females. dpp, days postpartum; exp., experiment.

Adult cKO ovaries exhibit blocked folliculogenesis

Because we obtained fully grown oocytes from antral follicles from 28 dpp cKO mice but fertility was severely compromised by 42 dpp, we analyzed the number of oocytes that could be collected from cKO females at different ages. Although there was no difference in the number of oocytes between cKO and B6 control

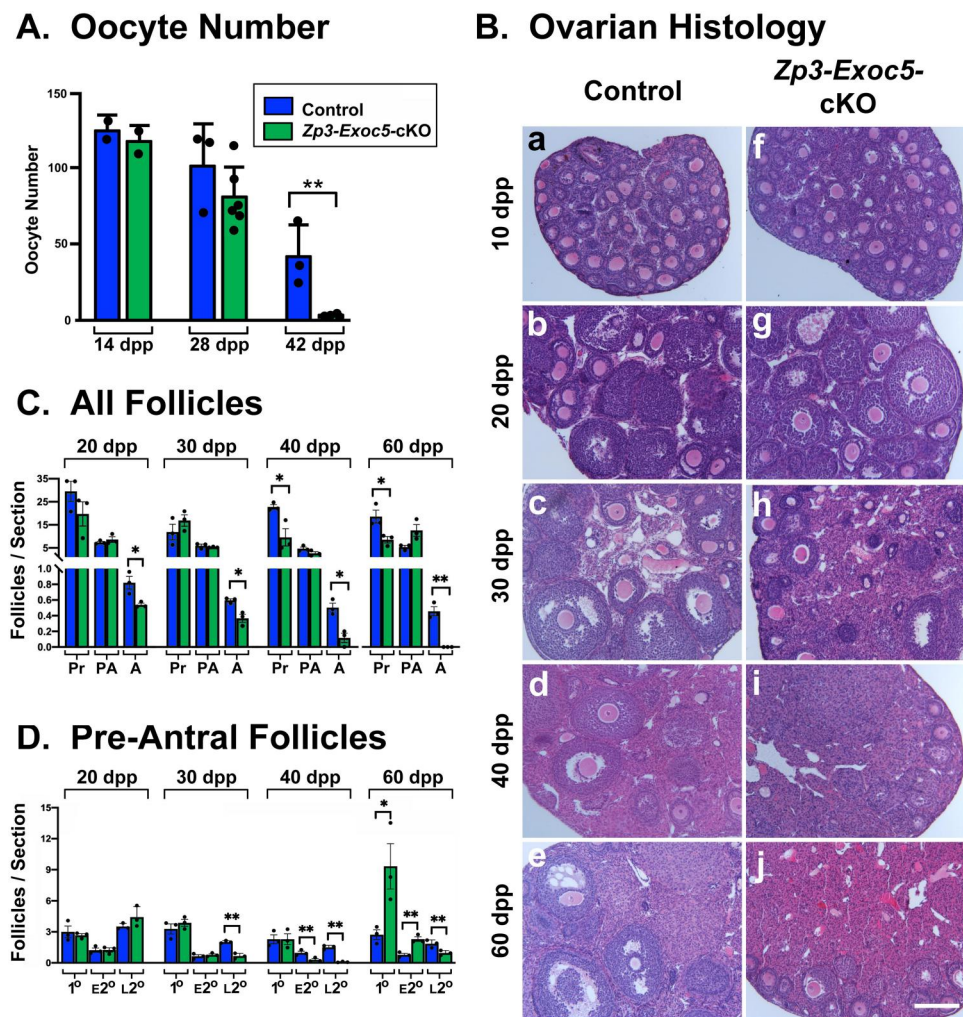


Figure 2. Follicles are depleted in knockout (cKO) mice. (A) Oocytes are depleted in cKO mice. Germinal vesicle (GV) oocytes were collected from control and cKO (*Zp3-Exoc5*-cKO) mice at different ages after birth and counted. cKO mice were statistically different only at 42-day postpartum (dpp). Error bars are SEM, and each point represents a single mouse. (B) Histological sections were prepared from control (B6 mice, a–e) ovaries and from cKO ovaries (f–j), from 10 to 60 dpp, and stained. Normal ovaries have visible antral follicles at all ages. All images are at the same magnification (bar = 0.2 mm). (C and D) Follicle dynamics of *Exoc5* deleted ovaries. Whole ovaries were serially sectioned at 5- μ m intervals, stained, and follicles were counted. Both ovaries from three different mice for each age group were counted for both cKO and control mice. (C) All follicles were divided into three groups, primordial (Pr), preantral (PA) including primary and secondary follicles, and antral (A) follicles. (D) Preantral follicles were divided into three groups, primary (1°), early secondary follicles with less than two full layers of granulosa cells (E2°), and late secondary follicles with two or more layers of granulosa cells (L2°). Representative images for secondary follicles in both groups are shown in [Supplementary Fig. S5](#). Differences between groups were analyzed for statistical significance (* $P < 0.05$; ** $P < 0.01$).

females prior to 28 dpp, we were unable to recover fully grown oocytes from adult female cKO (Fig. 2A). Thus, oocyte-specific deletion of *Exo5* causes infertility in adult females due to lack of production of fully grown oocytes. To better understand the infertility phenotype, we prepared histological sections of cKO and B6 control ovaries at six different ages spanning 10–60 dpp. Ovaries from cKO mice at 10 and 20 dpp were very similar to wild-type controls (Fig. 2Ba, b, f, and g). All follicle classes, including antral follicles, were present at similar numbers compared to controls (Fig. 2C). This is consistent with the observation that fully grown oocytes could be recovered at 28 dpp from cKO mice (Fig. 2A). By 30 dpp, atretic follicles were common in cKO ovaries (Fig. 2Bh). By 40 dpp, there were fewer preantral follicles and an accumulation of abnormal/atretic primary and secondary follicles. In these histological samples, there appeared to be a block in folliculogenesis at the secondary follicle stage (Fig. 2Bh). By 40 dpp, almost no antral follicles were present in cKO ovaries (Fig. 2Bi). These data suggest that the initial wave of

folliculogenesis could progress to the antral stage, but subsequent waves could not.

Folliculogenesis arrests at the secondary follicle stage

To better understand the dynamics of folliculogenesis, we classified and counted follicles at different stages of development in serially sectioned ovaries. We analyzed both ovaries from three mice in both control and cKO mice across ages (10, 20, 30, 40, and 60 days old) (Fig. 2C). Follicle numbers at all stages in cKO ovaries were not statistically different from those of controls up to 20 dpp, except there were a lower number of antral follicles in the cKO ovaries. This decrease in antral follicles became progressively more pronounced with age, with none being observed in cKO ovaries at 60 dpp. In addition to a decrease in antral follicles, there was a decrease in the number of primordial follicles (or ovarian reserve) at 40 and 60 dpp. These primordial follicles could have been lost via cell death mechanisms and/or via

activation. To better understand what may be occurring in pre-antral follicles, we further subdivided preantral follicles into primary follicles, early secondary follicles with less than two fully formed layers of granulosa cells surrounding the oocyte, and late secondary follicles with two or more layers of granulosa cells (Fig. 2D, Supplementary Fig. S5). The results show that preantral development appeared to be normal at 20 dpp, but by 60 dpp, most of the preantral follicles in cKO ovaries were primary or small secondary follicles, while control preantral follicles were more advanced in development. These data are consistent with a model in which the first wave of folliculogenesis is activated and progresses to the antral stage, and subsequent waves do not progress past the preantral stage.

Secondary and antral follicles in cKO mice undergo apoptosis

The gradual decrease in antral follicles from 30 dpp onwards suggested that the follicles were dying. We tested this by staining ovarian sections for DNA damage using the TUNEL Assay. We found that at 15 dpp, there was no measurable TUNEL signal in control mice (Fig. 3Aa), but this increased subsequently, as expected given that cell death is a natural process during folliculogenesis (Fig. 3Ac, e, and g) (Elvin et al., 1999; Hutt et al., 2006). In control secondary and antral follicles, TUNEL-positive cells were largely granulosa cells interspersed throughout the follicle or clustered near the developing antral cavity. In cKO follicles, the TUNEL-positive cells appeared later in development relative to

controls and were not visible until 28 dpp (Fig. 3Af and h). The positive TUNEL signal was more prominent in cKO follicles compared to controls. We quantified the TUNEL signal across age groups, and found that at 21 dpp, there was significantly less TUNEL signal in cKO follicles, but this drastically increased by 28 and 32 dpp (Fig. 3B). By 42 dpp, the TUNEL signal had largely decreased in *Zp3-Exoc5*-cKO.

All of the TUNEL-positive follicles that we found in both control and cKO ovaries were either secondary or antral follicles. When we replotted the total TUNEL intensity data by the type of follicle, we found that at 28 and 32 dpp, a much larger proportion of TUNEL-positive follicles in cKO ovaries were secondary, while in controls they were mostly antral (Fig. 3C and D). By 32 dpp, there was an increase in the intensity of TUNEL staining in cKO ovaries, as compared to controls, in both secondary and antral follicles, but the overall number of both had decreased. This is consistent with a loss of first-wave antral follicles and a loss of adult-wave secondary follicles at 28–32 dpp by apoptosis.

cKO ovaries appear fibrotic by early adulthood

Consistent with a decline in the number of primordial follicles and a loss of antral follicles, by 42 dpp, cKO ovaries appeared fibrotic with more stroma than follicles relative to controls. Reproductive aging is associated with a fibrotic milieu due to higher collagen content, so we stained cKO ovaries with PSR to detect collagen I and III. We found that starting as early as 28 dpp, there was a 2.7-fold increase in collagen in cKO ovaries

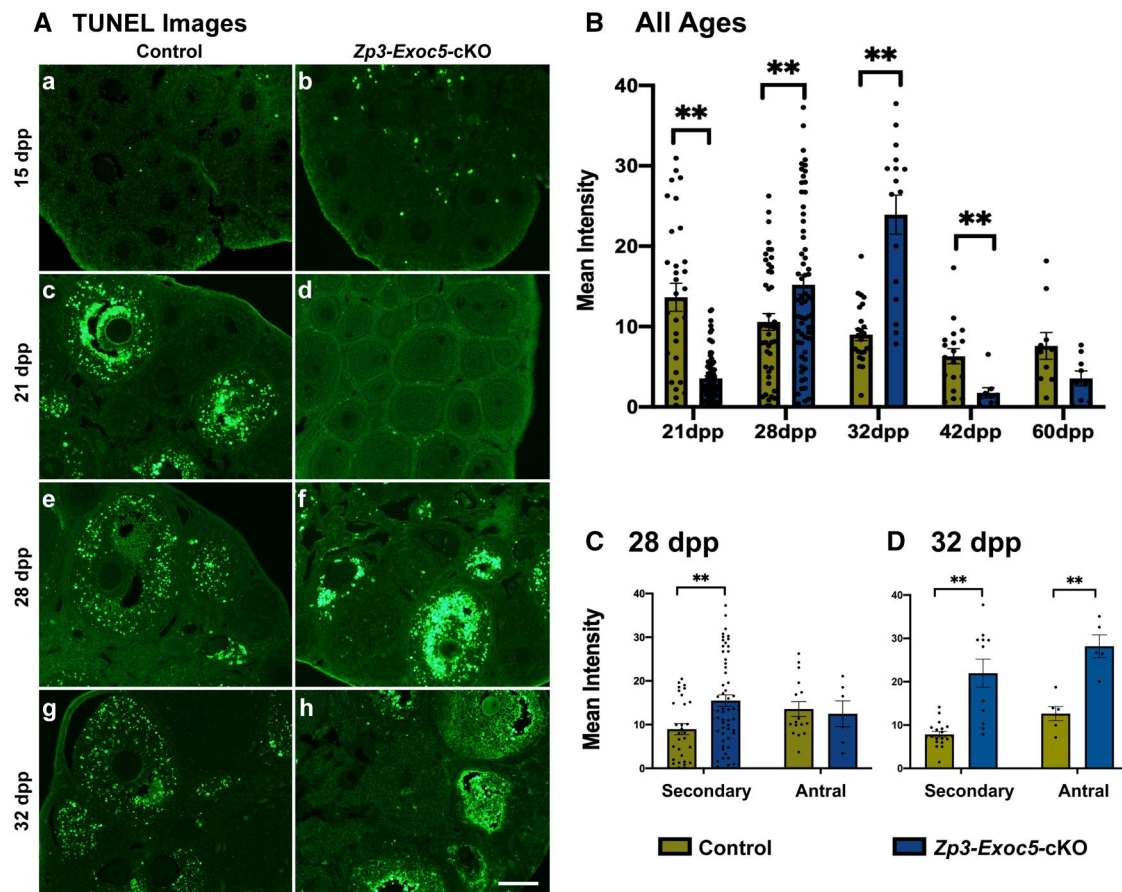


Figure 3. Follicles undergo apoptosis in response to *Exoc5* deletion. Whole ovaries of 15, 21, 28, and 32 dpp mice were serially sectioned at 5- μ m intervals and stained for apoptosis using TUNEL. (A) Examples of both control and knockout (cKO: *Zp3-Exoc5*-cKO) ovaries are shown. Bar = 100 μ m. (B and C) Secondary and antral follicles die at 28–32 dpp. TUNEL signals were quantitated as described. (B) TUNEL intensity for all follicles at all ages. At 21 dpp, there is less TUNEL positivity than for controls, but it increases at 28 and 32 dpp. (C) TUNEL intensity of follicles divided into small (secondary) and large (antral) follicles. (** $P < 0.01$)

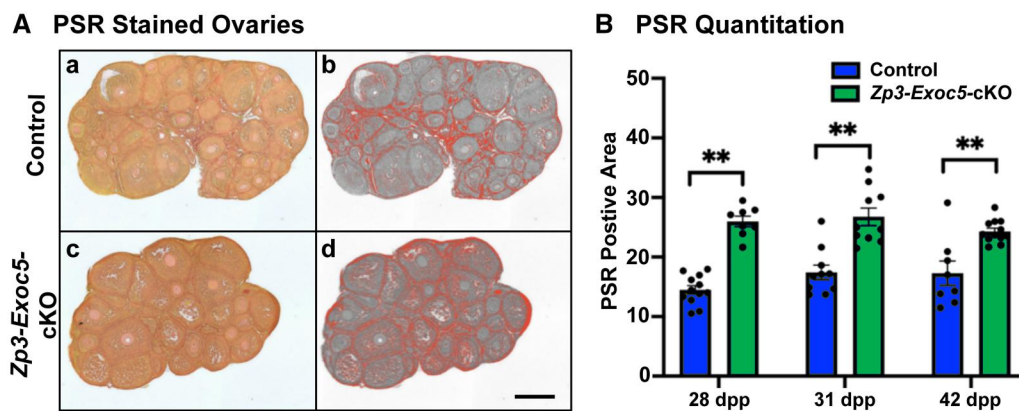


Figure 4. Collagen fiber deposition increased in knockout (cKO) ovaries. Collagen deposition was analyzed by staining whole ovary sections with picosirius red and quantitated. (A) Representative samples of PSR-stained ovaries for a control (a) and cKO (*Zp3-Exoc5-cKO*) (c) ovaries are shown. Processed color threshold images of a and c, respectively, are shown (b and d). Bar = 200 μ m. (B) Quantitation of images as described using ImageJ for different aged ovaries. Each dot in the graph represents one sectioned slide of an ovary. (** $P < 0.01$)

relative to controls which persisted across ages (Fig. 4). This suggested that fibrotic changes in the ovaries without EXOC5 in the oocytes were initiated early, even when oocytes were still present.

First-wave oocytes from cKO mice are developmentally compromised

Our data so far indicated that only the first wave of folliculogenesis progresses to the antral follicle stage. This, in turn, suggested that the first wave of folliculogenesis was not dependent on *Exoc5* expression. However, although the ovulated oocytes were morphologically indistinguishable from controls, including cumulus expansion, the oocytes could be functionally impaired. In normal mice, oocytes from the first wave of folliculogenesis do not mature past the antral follicle stage because of the hormonal milieu of the ovaries in prepubertal mice (Dullaart et al., 1975). However, when 21-day-old mice are stimulated with exogenous gonadotropins, antral follicles from the first wave continue to develop and produce eggs that, when fertilized, produce normal, healthy pups (Schroeder and Eppig, 1984). We tested whether the oocytes from the first wave of folliculogenesis of cKO ovaries were capable of developing to blastocysts in culture after IVF. We injected 21-day-old control and cKO females with gonadotropins to stimulate the maturation of antral follicles. These mice ovulated, and we were able to collect MII eggs, although cKO mice produced only about a third of the oocytes compared to normal controls (Supplementary Fig. S6). These MII eggs were incubated with control wild-type B6 sperm for IVF. cKO eggs had the same incidence of fertilization as controls, as measured by the percentage of eggs that progressed to 2-cell embryos (Supplementary Fig. S7). These embryos were then cultured for 120 h. Most (93.8%) of the control zygotes progressed to the hatching blastocyst stage, the final stage possible in culture under these conditions (Fig. 5A). Far fewer (24%) embryos generated from cKO mice reached the hatching stage and 68% of them died (Fig. 5B). These data suggest that cKO oocytes are developmentally incompetent.

cKO parthenogenotes cannot develop blastocoels

In the IVF experiment (Fig. 5), the newly created embryos would have EXOC5 because the paternal genome is activated at the 2-cell stage. Parthenogenetic activation of cKO MII oocytes allowed us to determine the effects of *Exoc5* deletion on embryogenesis without paternal contribution. We parthenogenetically activated cKO MII eggs and followed their development. We found that cKO

MII oocytes were very sensitive to activation in calcium-free media, which is the normal protocol we use for egg activation (Supplementary Fig. S8). Without Ca^{2+} , most of the cKO MII oocytes did not progress beyond the 2-cell stage and died shortly after activation with SrCl_2 . We also found that both control and cKO MII eggs progressed more efficiently in the presence of CB (Supplementary Figs S9 and S10). When control oocytes were parthenogenetically activated, most of them progressed to the blastocyst stage (Fig. 6A). When cKO MII oocytes were parthenogenetically activated, they could not form blastocysts with clear blastocoels (Fig. 6B). These embryos appeared normal at the morula stage, but then degenerated into a group of cells with some vacuoles (Supplementary Fig. S11). Occasionally, parthenogenetically generated cKO 2-cell embryos had large vacuoles in one of the two blastomeres (Supplementary Fig. S11C and D), a condition that is seen in cells without functioning exocyst complexes that are involved in forming large cavities (Bryant et al., 2010). These data indicate that without the EXOC5 provided by the paternal genome in IVF, parthenogenetically generated cKO embryos are severely compromised, and cannot form blastocoel cavities.

Discussion

Here we report that deletion of *Exoc5* in oocytes early in folliculogenesis inhibits folliculogenesis and results in two major phenotypes (Fig. 7). First, the first wave of folliculogenesis progresses to the antral stage but results in the production of oocytes whose developmental competence is compromised. Second, all subsequent waves of folliculogenesis in adult mice do not progress beyond the preantral stage due to increased cell death, and as a result, almost no antral follicles are present by 60 dpp. These two events lead to complete female infertility. The cKO mouse provides a novel model that is able to parse out the first and adult waves of folliculogenesis and help our understanding of the relationship between folliculogenesis and ovarian fibrosis, a hallmark of aging (Park et al., 2021). This model also elucidates a novel role of EXOC5 in folliculogenesis, which is likely related to cell-cell communication between the oocyte and its surrounding granulosa cells.

The phenotype in cKO ovaries differed greatly between the first and subsequent waves of folliculogenesis. In general, it is accepted that the first wave of folliculogenesis differs from subsequent adult waves in several respects (Zheng et al., 2014a,b).

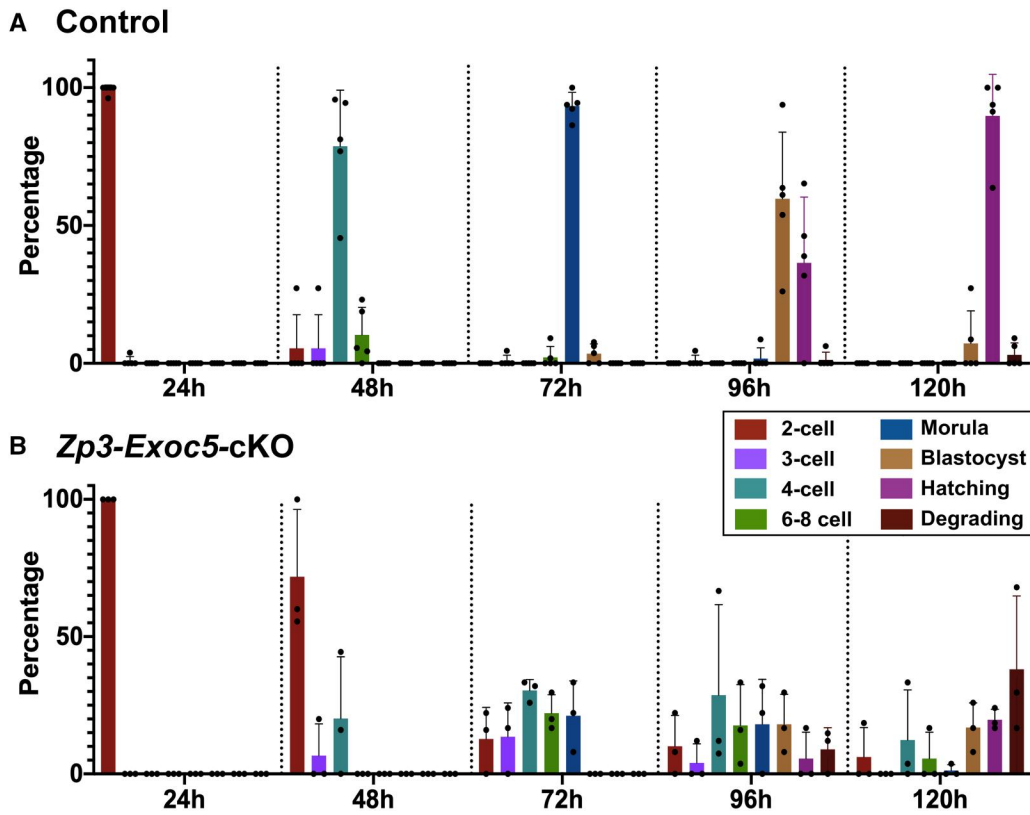


Figure 5. Knockout (cKO) oocytes are incompetent to undergo preimplantation embryogenesis. Control (A) and cKO (*Zp3-Exoc5-cKO*) (B) oocytes from gonadotropin-treated 21-day-old mice were fertilized *in vitro* with normal sperm and the resulting embryos were cultured for 120 h. The percentage of zygotes that progressed to each stage was measured at 24 h periods. Each point is one experiment with 20–30 oocytes. Error bars are SEM.

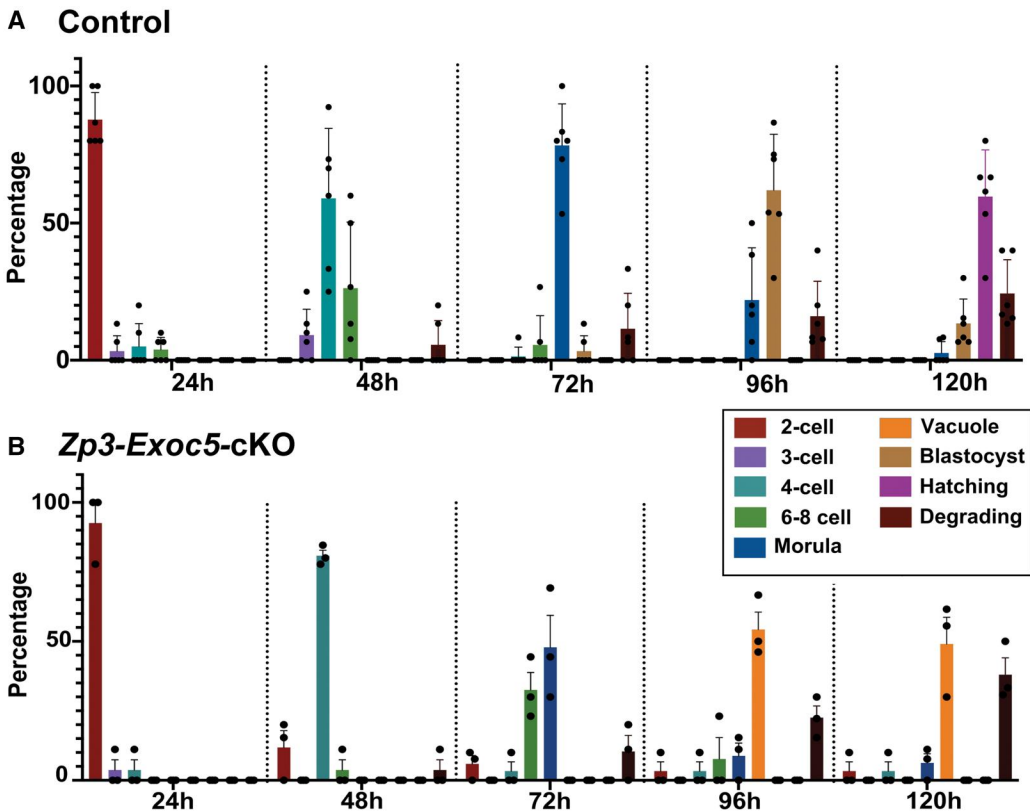


Figure 6. Parthenogenetic embryos created from knockout (cKO) oocytes have abnormal development. Control (A) and cKO (*Zp3-Exoc5-cKO*) (B) oocytes from gonadotropin-treated 21-day-old mice were treated with cytochalasin B, then parthenogenetically activated with SrCl₂. The resulting parthenogenotes were cultured for 120 h. The percentage of zygotes that progressed to each stage was measured at 24 h periods. Each point is one experiment with at least 10–20 oocytes. Error bars are SEM.

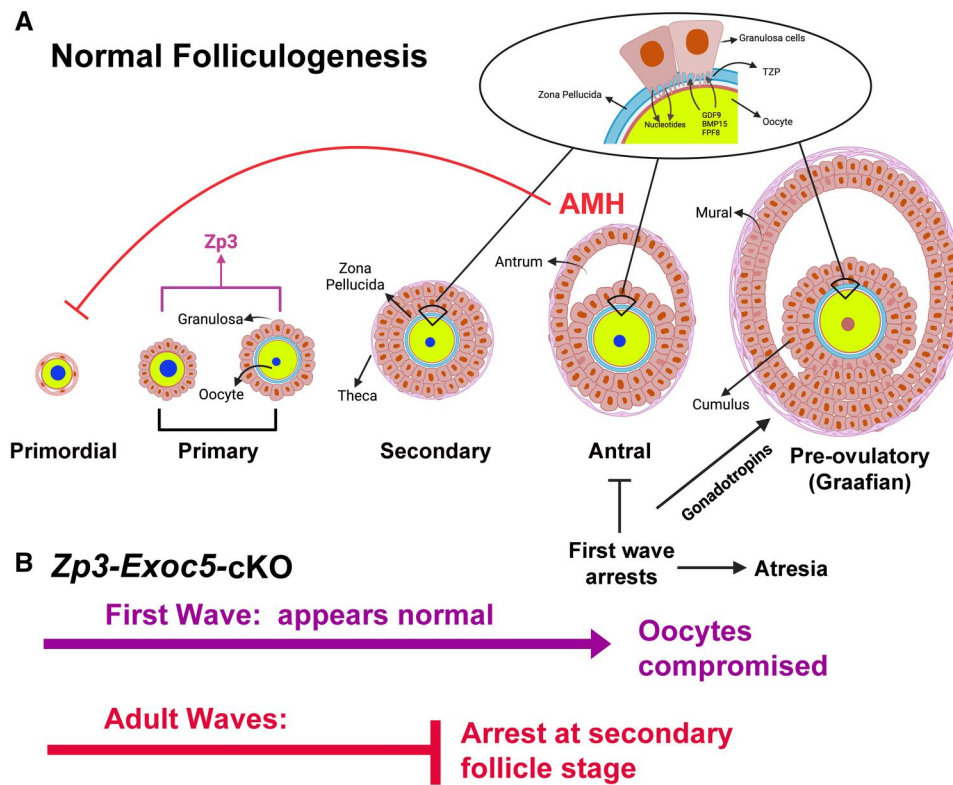


Figure 7. Model for the effect of *Exoc5* deletion on mouse folliculogenesis. (A) Normal folliculogenesis proceeds in two waves, both going through the same progression from the primordial reserve to mature follicles. (B) When *Exoc5* is selectively deleted from oocytes at the primary follicle stage, the first wave progresses to late antral follicles that die. The adult waves progress to the secondary follicle stage where they die.

Although there are currently no known markers that can clearly differentiate the first wave of folliculogenesis from subsequent ones, it is generally accepted that antral follicles in 21 dpp mice originate from the first wave which develops shortly after birth as soon as the follicles are formed. First-wave follicles in wild-type mice progress to the late antral stage, but then degenerate because the hormonal milieu of prepubertal mice is not yet fully supportive of follicular development (McGee and Hsueh, 2000). Although the physiologic relevance of the first-wave oocytes is not clear, at least one report has suggested that this population of oocytes can contribute to fertility for up to three months in the mouse (Zheng et al., 2014a). The origin of the supporting granulosa cells in these follicles is from the medulla (center) of the ovary, whereas all other follicles recruit granulosa cells from the cortex (periphery) of the ovary. Even with these differences, when 21 dpp mice are stimulated with exogenous gonadotropins, antral follicles from the first wave continue to develop and produce eggs that, when fertilized, can produce normal healthy pups (O'Brien et al., 2003), indicating that the first wave of folliculogenesis has the capacity to produce fully functional oocytes.

In our cKO mouse model, the first wave of folliculogenesis progresses to the antral stage, but the oocytes are not developmentally competent. Thus, the first wave of folliculogenesis requires EXOC5 for the production of developmentally competent oocytes, but not for the production of antral follicles. In the subsequent adult waves of folliculogenesis, the secondary and antral follicles appear to undergo apoptosis (as judged by TUNEL) and there are no antral follicles by 60 dpp, suggesting that adult follicular waves do require EXOC5 to progress to the antral stage. Our data do not suggest a mechanism for these clear differences in the effects of *Exoc5* deletion in first versus adult waves of folliculogenesis. It is possible that the first-wave antral follicles

cannot support the hormonal milieu required to allow subsequent waves to develop. But, activation of primordial follicles continues even up to 60 dpp, so some signaling remains intact. When all the data are considered collectively, it supports the model that the first and adult waves have different molecular responses to *Exoc5* deletion.

Bidirectional cell-cell communication between the granulosa cells and the oocyte in follicles is essential for folliculogenesis. This communication directs the granulosa cells to differentiate into mural and cumulus cells, to form the antral cavity, to direct the oocyte to grow, and to establish the supply of nutrients required for oocyte growth. The exocyst complex is a multi-subunit tethering complex that is required for fusion of secretory vesicles with the plasma membrane (Lepore et al., 2018). It is likely to be involved in different aspects of cell-cell communication in the follicle, including the secretion of oocyte-specific factors and the uptake of signals and nutrients in the oocyte from the granulosa cells. Deletion of *Exoc5* disrupts the entire exocyst complex and results in early embryonic lethality in mice when completely knocked out (Fogelgren et al., 2015). In the cKO mouse, *Exoc5* is only deleted in the oocytes and not in the granulosa cells. If, as we predict, EXOC5 is important for cell-cell communication in the follicle, this model emphasizes how closely the bidirectional communication between the two types of cells is regulated. It is clear from our results that the overwhelming phenotype is that all waves of folliculogenesis, except the first wave, are blocked and do not progress beyond the preantral stage. EXOC5 therefore appears to be essential for the earliest stages of folliculogenesis indicating that cell-cell communication between the two cell types is crucial for the earliest steps of folliculogenesis. Moreover, although the first wave of folliculogenesis can progress to the antral follicle stage in the cKO mice, it is important to

note that the resulting gamete quality is poor, suggesting that bidirectional communication may be compromised even in these follicles. Another possibility is that in the oocyte, EXOC5 may act independently from the exocyst complex in a way that we do not yet understand. This could be addressed indirectly by creating additional knockout mice with different components of the complex deleted.

Our results also demonstrated that EXOC5 is required for blastocoel formation because cKO parthenogenotes could not form them. The differentiation of the trophectoderm represents the body's first epithelia, with apical-basal polarization, tight junctions, and polarized exocytosis of fluid and electrolyte transporters. To form the blastocoel, these new epithelial cells require coordinated polarized trafficking of intracellular vesicles to a lumen-initiation site between adjacent cells to form the lumen (an epithelial morphogenesis process termed 'hollowing') (Bryant and Mostov, 2008). Previously published studies using MDCK epithelial cells cultured in collagen and matrigel substrates have shown that RNAi-based knockdown of exocyst subunits disrupted this process of cystogenesis (Lipschutz et al., 2000; Bryant et al., 2010; Polgar et al., 2015). Parthenogenotes develop to the blastocyst stage without any genetic input from paternal genes, so cKO parthenogenotes do not have any active *Exoc5* genes. While cKO parthenogenotes appear to develop normally to the morula stage, they cannot create the blastocoel. Instead, they begin to degenerate, often with smaller vacuoles between the cells or inside the cells, that is typical of cavity-forming organs that do not have functioning exocyst complexes (Bryant et al., 2010). These data suggest that EXOC5 is not required for development from the zygote to the morula but becomes important for the first clear cell differentiation that occurs at blastocyst formation. Finally, it is worth noting that antral follicles from the first wave in cKO ovaries are able to produce the antrum. This is probably because is the granulosa cells that produce this cavity, and they retain *Exoc5* in the cKO.

It is striking that *Exoc5* loss-of-function specifically in the growing oocyte can have such a profound and broad impact on the ovary. First, the microenvironment of cKO ovaries shows an accumulation of collagen that mimics the age-related increase in fibrosis (Briley et al., 2016; Amargant et al., 2020). It is possible that this fibrosis could be occurring as a result of an increased immune and inflammatory response needed to clear the large amount of cell death. Second, even though *Exoc5* is being deleted only in growing oocytes, there is clearly an indirect effect on primordial follicles, as there is a significant decrease in the ovarian reserve by 40 and 60 dpp. It is possible that the high levels of cell death in the cKO ovaries create an inhospitable milieu for primordial follicles and that they themselves die. Alternatively, and not mutually exclusively, it is possible that there is accelerated activation of the ovarian reserve due to decreased AMH resulting from the lack of large growing follicles in the cKO ovaries. Consistent with this possibility, we observed a large surge in primary and early secondary follicles at 60 dpp in the cKO ovaries. Studies are ongoing to determine the trajectory of ovarian fibrosis and how it might relate to aging in this model.

Our data establish that EXOC5 is required for folliculogenesis and may be important for the transition from morula to blastocyst. The first function emphasizes the role of EXOC5 in cell-cell communication between the oocyte and granulosa cells, because when this is disrupted, folliculogenesis is abruptly arrested. The second function emphasizes the role of EXOC5 in blastocoel cavity formation, which includes polarization of the embryonic cells. This model also emphasizes the tight integration between

folliculogenesis and a healthy ovarian environment. When folliculogenesis is prematurely arrested, the ovaries age precociously. Finally, this model provides a unique method to isolate the first wave of folliculogenesis from adult waves, since only the first wave progresses to the antral stage. The cKO mouse therefore provides an important new tool to study three aspects of folliculogenesis: the bidirectional cell-cell communication, the differences between the first and all subsequent waves of folliculogenesis, and the relationship between folliculogenesis and ovarian fibrosis.

Supplementary data

Supplementary data are available at *Molecular Human Reproduction* online.

Data availability

Original data will be made available upon request.

Acknowledgements

The authors would like to thank Dr John Eppig for many useful discussions during the course of this work. His expertise and suggestions formulated many of our experiments and thinking along the way. The authors would like to thank Dr Farners Amargant and Cosmo Hahn for technical support, and Dr Jennifer McKey for valuable discussions.

Authors' roles

H.W. performed the bulk of the experiments at the University of Hawaii and provided intellectual contributions. H.N. and P.H.H. both provided technical expertise and experimental support. B.F. provided expertise on EXOC5 and assisted with breeding. F.E.D. and W.S.W. led the project, designed the experiments, and directed the work.

Funding

NIH (R01HD105752 to F.E.D.); Transgenic Core (GM13144 to W.S.W.; R01GM123048 to W.S.W.); Hawaii Community Foundation (MedRes 2022 000000563 to W.S.W.).

Conflict of interest

None declared.

References

- Amargant F, Manuel SL, Tu Q, Parkes WS, Rivas F, Zhou LT, Rowley JE, Villanueva CE, Hornick JE, Shekhawat GS et al. Ovarian stiffness increases with age in the mammalian ovary and depends on collagen and hyaluronan matrices. *Aging Cell* 2020;**19**:e13259.
- Briley SM, Jasti S, McCracken JM, Hornick JE, Fegley B, Pritchard MT, Duncan FE. Reproductive age-associated fibrosis in the stroma of the mammalian ovary. *Reproduction* 2016;**152**:245–260.
- Bryant DM, Datta A, Rodriguez-Fraticelli AE, Peranen J, Martin-Belmonte F, Mostov KE. A molecular network for de novo generation of the apical surface and lumen. *Nat Cell Biol* 2010;**12**:1035–1045.
- Bryant DM, Mostov KE. From cells to organs: building polarized tissue. *Nat Rev Mol Cell Biol* 2008;**9**:887–901.

- Channing CP, Schaerf FW, Anderson LD, Tsafiri A. Ovarian follicular and luteal physiology. *Int Rev Physiol* 1980;**22**:117–201.
- Clarke HJ. History, origin, and function of transzonal projections: the bridges of communication between the oocyte and its environment. *Anim Reprod* 2018a;**15**:215–223.
- Clarke HJ. Regulation of germ cell development by intercellular signaling in the mammalian ovarian follicle. *Wiley Interdiscip Rev Dev Biol* 2018b;**7**:10.1002/wdev.294.
- de Vries WN, Binns LT, Fancher KS, Dean J, Moore R, Kemler R, Knowles BB. Expression of Cre recombinase in mouse oocytes: a means to study maternal effect genes. *Genesis* 2000;**26**:110–112.
- Dullaart J, Kent J, Ryle M. Serum gonadotrophin concentrations in infantile female mice. *J Reprod Fertil* 1975;**43**:189–192.
- Duncan FE, Jasti S, Paulson A, Kelsh JM, Fegley B, Gerton JL. Age-associated dysregulation of protein metabolism in the mammalian oocyte. *Aging Cell* 2017;**16**:1381–1393.
- Elvin JA, Yan C, Wang P, Nishimori K, Matzuk MM. Molecular characterization of the follicle defects in the growth differentiation factor 9-deficient ovary. *Mol Endocrinol* 1999;**13**:1018–1034.
- Fogelgren B, Lin SY, Zuo X, Jaffe KM, Park KM, Reichert RJ, Bell PD, Burdine RD, Lipschutz JH. The exocyst protein Sec10 interacts with Polycystin-2 and knockdown causes PKD-phenotypes. *PLoS Genet* 2011;**7**:e1001361.
- Fogelgren B, Polgar N, Lui VH, Lee AJ, Tamashiro KK, Napoli JA, Walton CB, Zuo X, Lipschutz JH. Urothelial defects from targeted inactivation of Exocyst Sec10 in mice cause ureteropelvic junction obstructions. *PLoS One* 2015;**10**:e0129346.
- Friedrich GA, Hildebrand JD, Soriano P. The secretory protein Sec8 is required for paraxial mesoderm formation in the mouse. *Dev Biol* 1997;**192**:364–374.
- Fujimoto BA, Young M, Carter L, Pang APS, Corley MJ, Fogelgren B, Polgar N. The exocyst complex regulates insulin-stimulated glucose uptake of skeletal muscle cells. *Am J Physiol Endocrinol Metab* 2019;**317**:E957–E972.
- Fujimoto BA, Young M, Nakamura N, Ha H, Carter L, Pitts MW, Torres D, Noh HL, Suk S, Kim JK et al. Disrupted glucose homeostasis and skeletal-muscle-specific glucose uptake in an exocyst knockout mouse model. *J Biol Chem* 2021;**296**:100482.
- Fulmer D, Toomer K, Guo L, Moore K, Glover J, Moore R, Stairley R, Lobo G, Zuo X, Dang Y et al. Defects in the exocyst-cilia machinery cause bicuspid aortic valve disease and aortic stenosis. *Circulation* 2019;**140**:1331–1341.
- Hutt KJ, McLaughlin EA, Holland MK. Primordial follicle activation and follicular development in the juvenile rabbit ovary. *Cell Tissue Res* 2006;**326**:809–822.
- Kerr JB, Duckett R, Myers M, Britt KL, Mladenovska T, Findlay JK. Quantification of healthy follicles in the neonatal and adult mouse ovary: evidence for maintenance of primordial follicle supply. *Reproduction* 2006;**132**:95–109.
- Lee AJ, Polgar N, Napoli JA, Lui VH, Tamashiro KK, Fujimoto BA, Thompson KS, Fogelgren B. Fibroproliferative response to urothelial failure obliterates the ureter lumen in a mouse model of prenatal congenital obstructive nephropathy. *Sci Rep* 2016;**6**:31137.
- Lee B, Baek JI, Min H, Bae SH, Moon K, Kim MA, Kim YR, Fogelgren B, Lipschutz JH, Lee KY et al. Exocyst complex member EXOC5 is required for survival of hair cells and spiral ganglion neurons and maintenance of hearing. *Mol Neurobiol* 2018;**55**:6518–6532.
- Lepore DM, Martinez-Nunez L, Munson M. Exposing the elusive exocyst structure. *Trends Biochem Sci* 2018;**43**:714–725.
- Lewandoski M, Wassarman KM, Martin GR. Zp3-cre, a transgenic mouse line for the activation or inactivation of loxP-flanked target genes specifically in the female germ line. *Curr Biol* 1997;**7**:148–151.
- Lipschutz JH, Guo W, O'Brien LE, Nguyen YH, Novick P, Mostov KE. Exocyst is involved in cystogenesis and tubulogenesis and acts by modulating synthesis and delivery of basolateral plasma membrane and secretory proteins. *Mol Biol Cell* 2000;**11**:4259–4275.
- Livak KJ, Schmittgen TD. Analysis of relative gene expression data using real-time quantitative PCR and the 2(-Delta C(T)) method. *Methods* 2001;**25**:402–408.
- Lobo GP, Fulmer D, Guo L, Zuo X, Dang Y, Kim SH, Su Y, George K, Obert E, Fogelgren B et al. The exocyst is required for photoreceptor ciliogenesis and retinal development. *J Biol Chem* 2017;**292**:14814–14826.
- Matzuk MM, Burns KH, Viveiros MM, Eppig JJ. Intercellular communication in the mammalian ovary: oocytes carry the conversation. *Science* 2002;**296**:2178–2180.
- McGee EA, Hsueh AJ. Initial and cyclic recruitment of ovarian follicles. *Endocr Rev* 2000;**21**:200–214.
- Nguyen H, Wu H, Ung A, Yamazaki Y, Fogelgren B, Ward WS. Deletion of Orc4 during oogenesis severely reduces polar body extrusion and blocks zygotic DNA replication. *Biol Reprod* 2022;**106**:730–740.
- Nihalani D, Solanki AK, Arif E, Srivastava P, Rahman B, Zuo X, Dang Y, Fogelgren B, Fermin D, Gillies CE et al. Disruption of the exocyst induces podocyte loss and dysfunction. *J Biol Chem* 2019;**294**:10104–10119.
- Norris RP, Ratzan WJ, Freudzon M, Mehlmann LM, Krall J, Movsesian MA, Wang H, Ke H, Nikolaev VO, Jaffe LA. Cyclic GMP from the surrounding somatic cells regulates cyclic AMP and meiosis in the mouse oocyte. *Development* 2009;**136**:1869–1878.
- Novick P, Field C, Schekman R. Identification of 23 complementation groups required for post-translational events in the yeast secretory pathway. *Cell* 1980;**21**:205–215.
- Novick P, Schekman R. Secretion and cell-surface growth are blocked in a temperature-sensitive mutant of *Saccharomyces cerevisiae*. *Proc Natl Acad Sci USA* 1979;**76**:1858–1862.
- O'Brien MJ, Pendola JK, Eppig JJ. A revised protocol for in vitro development of mouse oocytes from primordial follicles dramatically improves their developmental competence. *Biol Reprod* 2003;**68**:1682–1686.
- Park SU, Walsh L, Berkowitz KM. Mechanisms of ovarian aging. *Reproduction* 2021;**162**:R19–R33.
- Peters H. The development of the mouse ovary from birth to maturity. *Acta Endocrinol (Copenh)* 1969;**62**:98–116.
- Peters H, Byskov AG, Himelstein-Braw R, Faber M. Follicular growth: the basic event in the mouse and human ovary. *J Reprod Fertil* 1975;**45**:559–566.
- Ploutarchou P, Melo P, Day AJ, Milner CM, Williams SA. Molecular analysis of the cumulus matrix: insights from mice with O-glycan-deficient oocytes. *Reproduction* 2015;**149**:533–543.
- Polgar N, Fogelgren B. Regulation of cell polarity by exocyst-mediated trafficking. *Cold Spring Harb Perspect Biol* 2018;**10**:a031401.
- Polgar N, Lee AJ, Lui VH, Napoli JA, Fogelgren B. The exocyst gene Sec10 regulates renal epithelial monolayer homeostasis and apoptotic sensitivity. *Am J Physiol Cell Physiol* 2015;**309**:C190–C201.
- Rohrer B, Biswal MR, Obert E, Dang Y, Su Y, Zuo X, Fogelgren B, Kondkar AA, Lobo GP, Lipschutz JH. Conditional loss of the exocyst component Exoc5 in retinal pigment epithelium (RPE) results in RPE dysfunction, photoreceptor cell degeneration, and decreased visual function. *Int J Mol Sci* 2021;**22**:5083.
- Schmittgen TD, Livak KJ. Analyzing real-time PCR data by the comparative C(T) method. *Nat Protoc* 2008;**3**:1101–1108.
- Schroeder AC, Eppig JJ. The developmental capacity of mouse oocytes that matured spontaneously in vitro is normal. *Dev Biol* 1984;**102**:493–497.

- Su YQ, Sugiura K, Wigglesworth K, O'Brien MJ, Affourtit JP, Pangas SA, Matzuk MM, Eppig JJ. Oocyte regulation of metabolic cooperativity between mouse cumulus cells and oocytes: BMP15 and GDF9 control cholesterol biosynthesis in cumulus cells. *Development* 2008;**135**:111–121.
- Su YQ, Wu X, O'Brien MJ, Pendola FL, Denegre JN, Matzuk MM, Eppig JJ. Synergistic roles of BMP15 and GDF9 in the development and function of the oocyte-cumulus cell complex in mice: genetic evidence for an oocyte-granulosa cell regulatory loop. *Dev Biol* 2004;**276**:64–73.
- Sugiura K, Eppig JJ. Society for Reproductive Biology Founders' Lecture 2005. Control of metabolic cooperativity between oocytes and their companion granulosa cells by mouse oocytes. *Reprod Fertil Dev* 2005;**17**:667–674.
- Sugiura K, Pendola FL, Eppig JJ. Oocyte control of metabolic cooperativity between oocytes and companion granulosa cells: energy metabolism. *Dev Biol* 2005;**279**:20–30.
- Sun QY, Liu K, Kikuchi K. Oocyte-specific knockout: a novel in vivo approach for studying gene functions during folliculogenesis, oocyte maturation, fertilization, and embryogenesis. *Biol Reprod* 2008;**79**:1014–1020.
- Wang F, Flanagan J, Su N, Wang LC, Bui S, Nielson A, Wu X, Vo HT, Ma XJ, Luo Y. RNAscope: a novel in situ RNA analysis platform for formalin-fixed, paraffin-embedded tissues. *J Mol Diagn* 2012;**14**:22–29.
- Yeaman C, Grindstaff KK, Nelson WJ. Mechanism of recruiting Sec6/8 (exocyst) complex to the apical junctional complex during polarization of epithelial cells. *J Cell Sci* 2004;**117**:559–570.
- Zheng W, Zhang H, Gorre N, Risal S, Shen Y, Liu K. Two classes of ovarian primordial follicles exhibit distinct developmental dynamics and physiological functions. *Hum Mol Genet* 2014a;**23**:920–928.
- Zheng W, Zhang H, Liu K. The two classes of primordial follicles in the mouse ovary: their development, physiological functions and implications for future research. *Mol Hum Reprod* 2014b;**20**:286–292.
- Zuo X, Guo W, Lipschutz JH. The exocyst protein Sec10 is necessary for primary ciliogenesis and cystogenesis in vitro. *Mol Biol Cell* 2009;**20**:2522–2529.